

Supplementary data for

Adaptive control of saccades via internal feedback

Haiyin Chen-Harris, Wilsaan M. Joiner, Vincent Ethier,

David S. Zee, and Reza Shadmehr

Results of Control Experiment 2: In this control study, target jumps were random – T1 had an equal chance of jumping up or down during the initial saccade. We found that the primary saccades were straight and showed no detectable bias in their endpoint toward the direction of the target jump (Fig. S1).

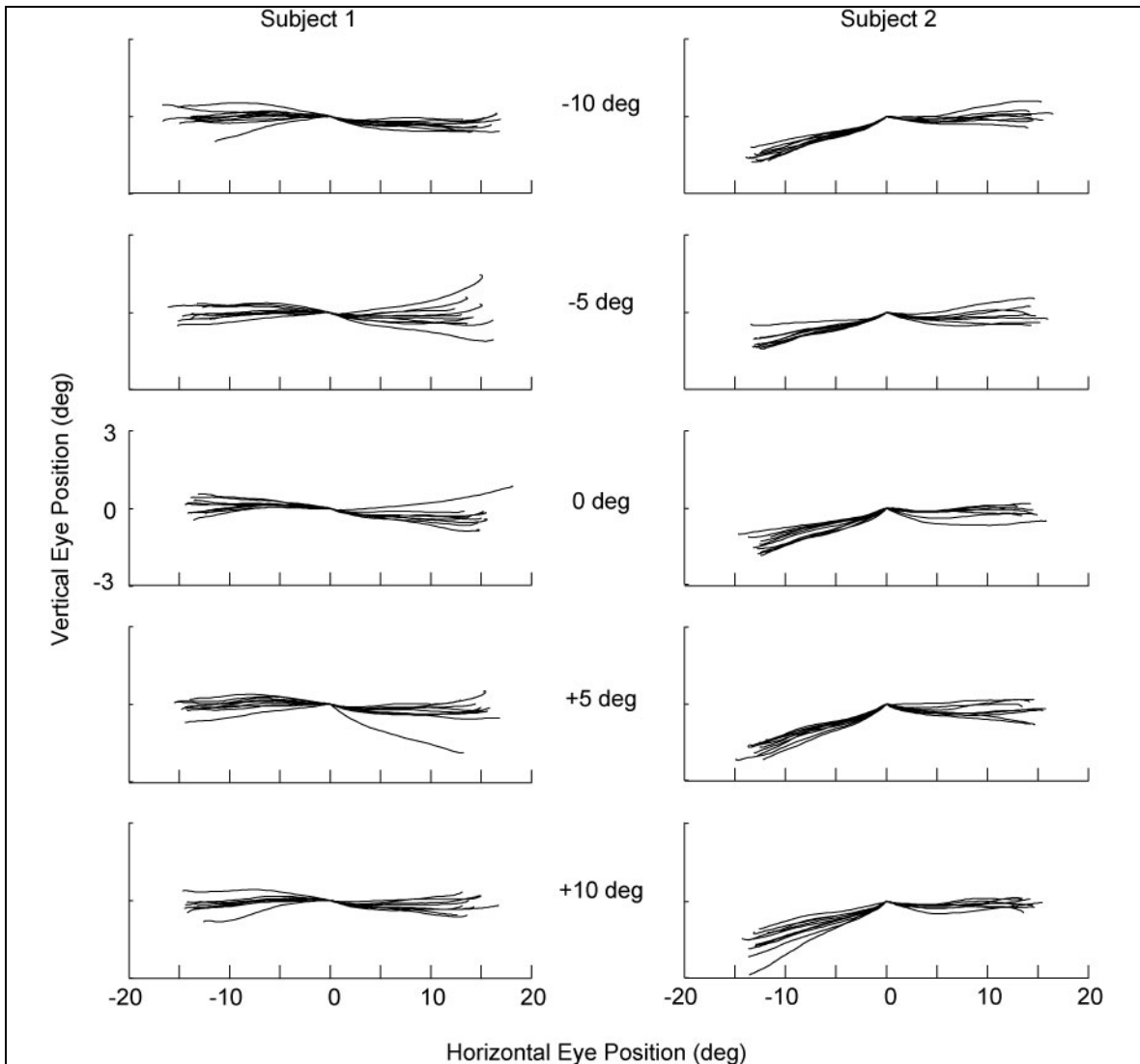


Figure S1. Random target jumps did not induce adaptation or curvature.

Individual saccades made during the random target jump experiment by two subjects. Trials are sorted and grouped according to the vertical target step size. A positive step indicates a target jump along the positive y-axis.

Modeling Cross-axis Saccade Adaptation

1. Distributing error among two likely sources

To model trial-to-trial adaptation, we began with endpoint error. At the end of a saccade in trial n , if the target was visible, i.e., trial n was not a catch trial, then retinal error was observed: $\mathbf{y}^{(n)} = \mathbf{r}^{(n)} - \mathbf{e}^{(n)}$. This error could be due to an error in the expected position of the target, $\tilde{\mathbf{r}}^{(n)}$, or an error in the expected final position of the eyes, $\tilde{\mathbf{e}}^{(n)}$:

$$\mathbf{y}^{(n)} = \tilde{\mathbf{r}}^{(n)} + \tilde{\mathbf{e}}^{(n)} \quad (\text{S1})$$

This posed a credit assignment problem – how does the brain distribute the total observed error across the two likely sources? We posited that the bigger the retinal error, the more likely the brain attributed the error in its expectation of target position, i.e., the target had moved during the saccade. Using the binary random variable q to specify whether the target had jumped or not, we wrote the probability of this jump as a logistic function:

$$P(q=1) = \left(1 + \exp\left(k\sigma - ky^{(n)}\right)\right)^{-1} \quad (\text{S2})$$

While in Eq. (S1) the endpoint error is a vector, in Eq. (S2) it is a scalar that represents the vertical component of the error (as the target jumps were along the vertical axis). We then used this probability to assign error to target movement:

$$\tilde{\mathbf{r}}^{(n)} = \mathbf{y}^{(n)} P(q=1) \quad (\text{S3})$$

The remainder of the total error was assigned to $\tilde{\mathbf{e}}^{(n)}$. At the end of each trial, the forward model updated its expected position of the target for the next saccade:

$$\hat{\mathbf{r}}^{(n+1)} = (1 - a_r)\hat{\mathbf{r}}^{(n)} + b_r\tilde{\mathbf{r}}^{(n)} \quad (\text{S4})$$

Note that this adaptive response has a single timescale, specified by forgetting rate a_r and learning rate b_r .

2. Implementing cross-axis adaptation by coupling the vertical and the horizontal saccade systems

To respond to the error in eye position, the forward model updated its model of dynamics of the eyes, \hat{B} . In the cross-axis adaptation experiment, the subject observed a vertical undershoot whenever a horizontal motor command was issued. To correct for this error, forward model's predictions about the behaviors of horizontal and vertical saccadic systems may gradually become coupled. To model this, we changed the term \hat{B} to include a “cross-coupling” term, g :

$$\hat{B}^{(n+1)} = B + \begin{bmatrix} 0 & 0 & 0 & -g^{(n)}(\tau_1\tau_2)^{-1} & 0 & 0 & 0 & 0 \\ 0 & 0 & 0 & 0 & 0 & 0 & 0 & 0 \end{bmatrix}^T \quad (\text{S5})$$

(The constants, τ_1 and τ_2 , were the same as in system matrix A and B .) Eq. (S5) describes a forward model that predicts a downward vertical movement whenever a horizontal motor commands is made. For the saccades to remain straight, the system matrix B used by the control policy would have to change to precisely match \hat{B} . Otherwise, as shown in Fig. 2D, saccade trajectories will become curved.

The learning of parameter g was supported by two timescales (Smith et al., 2006):

$$\begin{aligned} g^{(n)} &= g_{fast}^{(n)} + g_{slow}^{(n)} \\ g_{fast}^{(n+1)} &= (1 - a_{fast})g_{fast}^{(n)} + b_{fast}\tilde{e}_y^{(n)} \\ g_{slow}^{(n+1)} &= (1 - a_{slow})g_{slow}^{(n)} + b_{slow}\tilde{e}_y^{(n)} \end{aligned} \quad (\text{S6})$$

It has been shown that when feedback regarding saccade accuracy is withheld for more than 600ms, adaptation is abolished (Fujita et al., 2002). In our experiment, catch trials withheld sensory feedback by about 700ms. Therefore, we assumed zero error for all catch trials, which meant in the model, g and \hat{r} decayed on catch trials. We simulated each of the short breaks between sets with 5 additional catch trials.

In total, our model contained 8 parameters: $a_r, b_r, a_{fast}, b_{fast}, a_{slow}, b_{slow}, \sigma$, and k . We simulated 540 primary saccade trajectories: 480 adaptation trials and 60 post-adaptation catch trials. Three measurements from each simulated trajectory was taken for data fitting: the first and the fourth chord slopes (S1 and S4), and the vertical endpoint. To find the 8 parameter values, we used nonlinear least-squares solver (Matlab, Mathworks Inc.) to fit the 1620 metrics from simulation to the corresponding values from the actual data (average data of 11 subjects). The goodness of fit for the model was evaluated with the statistic r^2 , the fraction of the observed variance accounted for by our model compared to that by the null model (mean of the data), and the statistic χ^2 , the sum of squared-ratio between residual and measurement uncertainty, where standard deviation across subjects was used as the uncertainty about the mean.

In Fig. 2D, we also considered the effects of changes in the control policy. To adapt the control policy, we simply changed B in Eq. (2) and recomputed the feedback gains.

3. Model parameters

The A and B matrices used in Eq. (2) were:

$$A = \begin{bmatrix} 0.9998 & 0.00096 & 0 & 0 & 0 & 0 \\ -0.329 & 0.922 & 0 & 0 & 0 & 0 \\ 0 & 0 & 0.9998 & 0.00096 & 0 & 0 \\ 0 & 0 & -0.329 & 0.922 & 0 & 0 \\ 0 & 0 & 0 & 0 & 1 & 0 \\ 0 & 0 & 0 & 0 & 0 & 1 \end{bmatrix}$$

$$B = \begin{bmatrix} 0.000167 & 0.33 & 0 & 0 & 0 & 0 \\ 0 & 0 & 0.000167 & 0.33 & 0 & 0 \end{bmatrix}^T$$

Results of Optimal Feedback Control Model

We took the first steps to represent some of the changes that we had seen in the saccade trajectories using the mathematical framework of optimal control. Our work highlighted a fundamental problem: are the endpoint errors due to changes in the oculomotor plant, or due to changes in the sensory coding of the target? We will suggest that curvature arises only when errors are attributed to the oculomotor plant.

We will not explicitly model fatigue, partly because at this point it is not clear what causes it: is it due to fatigue in some of the neurons that generate the motor commands, or a general arousal state of the brain? Instead, we will focus on the adaptation that the system showed in response to the endpoint errors. That is, changes that occurred in chord slopes. In all the simulations reported below we kept $\alpha = 0.03$ and assumed a constant saccade duration of 65ms.

The rules of error-assignment are revealed by two sigmoid functions in Fig. S2A. At the start of training, when the endpoint errors were relatively large, the model attributed nearly all of the error to target jump (Fig. S2B), resulting in fairly large changes in S1 and only modest curvature. As training proceeded and the errors became smaller, a larger fraction of the error was assigned to drive adaptation of the forward model of the oculomotor plant (Fig. S2B), thereby producing increasing curvature (Fig. S2C). We fit two learning and forgetting rates to the forward model of the eye and one rate to the target remapping. The resulting model was able to capture the intricate temporal dynamics in our data (Fig. S2E&F, goodness of fit for all data points: $r^2 = 0.829$, reduced $\chi^2 = 1.892$). We found the learning rates for the fast and slow system of the forward model to be 0.104 and 0.000896, respectively, and the forgetting rates 1 (complete forgetting) and 0.0260, respectively. The learning and forgetting rates for the internal goal were 0.00147 and 0.00189, respectively. Fig. S2G displays the progression of chord slopes of the simulated saccade trajectories in the same format as in Fig. 3, demonstrating the effectiveness of

the error-assignment model. Simulation of a model in which error drove the forward model of the eye plant and target jump equally did not produce nearly the same quality of fit: $r^2 = 0.574$, reduced $\chi^2 = 4.64$.

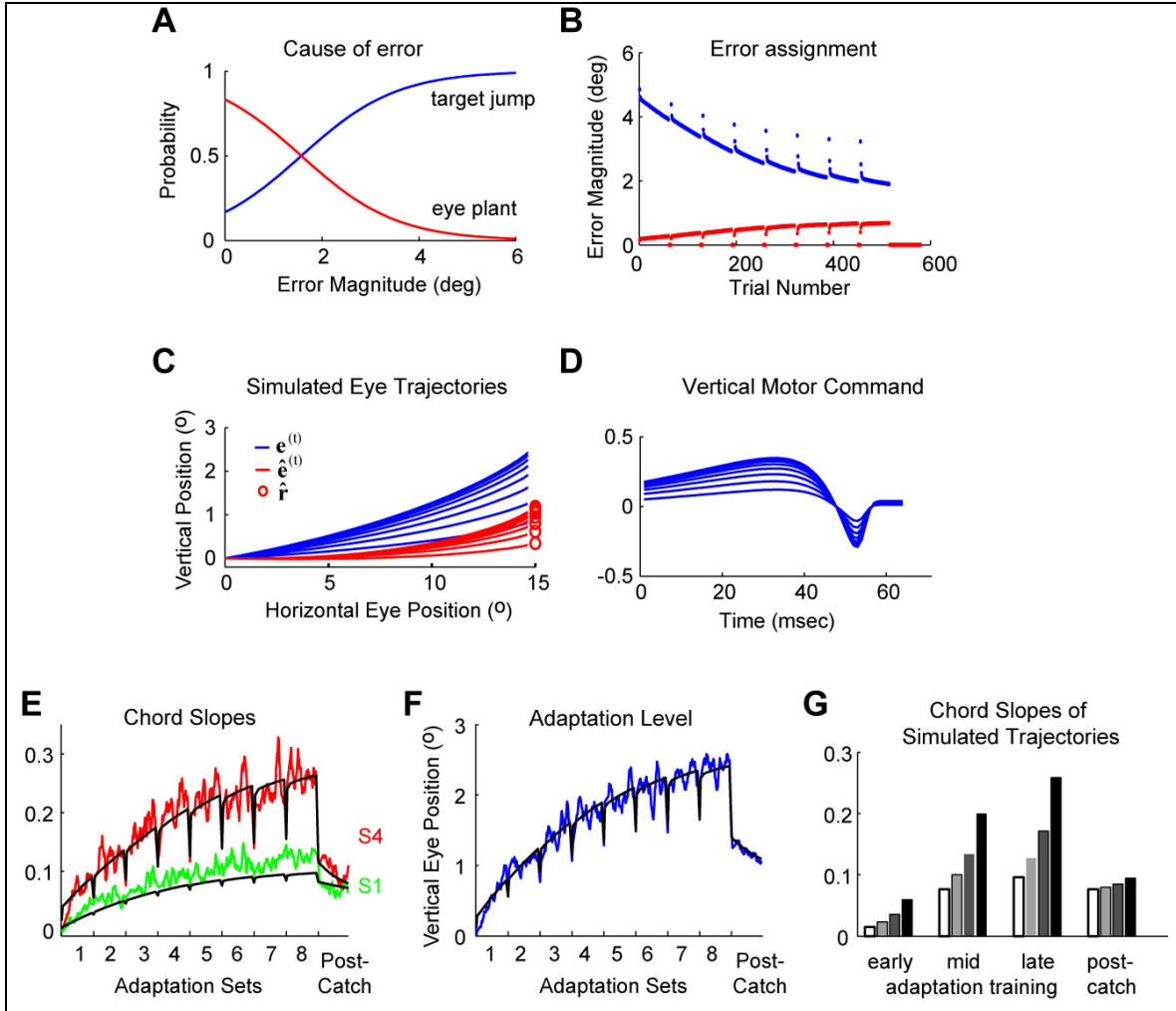


Figure S2. Adaptation of the optimal feedback control model.

A. Cause of error: when saccade endpoint produces a retinal error, the model assigns a probability to the cause of the error. The larger the endpoint error, the larger the probability that it was caused by an intra-saccadic jump in the target position. **B.** The magnitude of error attributed to target jump (blue) or changes to the oculomotor plant (red) throughout the adaptation experiment. Only near the end of the adaptation trials, when errors become small, we see errors credited to changes in the plant. **C.** Saccade trajectories produced by the model on the last trial of each training set and the last trial of the post-training catch trial set. The blue lines represent actual eye position $\mathbf{e}^{(t)}$. Red lines are estimated eye positions $\hat{\mathbf{e}}^{(t)}$. The red circle is estimated target position (that is, the remapped position $\hat{\mathbf{r}}$). **D.** Vertical component of the motor commands produced for the trials displayed in part C. **E.** Initial and final chord slopes (S1 and S4) of simulated saccades (black) overlaid on experimental results (red and green) across 11 subjects. **F.** Vertical endpoint of simulated saccades (black) overlaid on experimental results (blue). **G.** Average chord slopes of the simulated saccades at various stages of the experiment. The gray bars

correspond to chord slopes S1, S2, S3 and S4, with the darkest bar corresponding to S4.

Reference List

Fujita M, Amagai A, Minakawa F, Aoki M (2002) Selective and delay adaptation of human saccades. *Brain Res Cogn Brain Res* 13:41-52.

Smith MA, Ghazizadeh A, Shadmehr R (2006) Interacting adaptive processes with different timescales underlie short-term motor learning. *PLoS Biol* 4:e179.